Design of a multi-standard IR-UWB emitter in a 28 nm FD-SOI technology based on the frequency transposition pulse synthesis

Felipe Artemio Schoulten, Rémy Vauché, Jean Gaubert, Sylvain Bourdel, André Augusto Mariano

Design of a multi-standard IR-UWB emitter in a 28 nm FD-SOI technology based on the frequency transposition pulse synthesis

F. A. Schoulten[1], R. Vauche[1], J. Gaubert [1], S. Bourdel[2], and A. A. Mariano[3]

[1] Aix Marseille Univ, CNRS, IM2NP, Marseille, France
[2] TIMA, Université Grenoble-Alpes, Grenoble-INP, Grenoble, France
[3] GICS-UFPR, Universidade Federal do Parana, Curitiba, Brazil
e-mail: felipe.artemio-schoulten@univ-amu.fr

***Abstract*— Ultra-WideBand Impulse Radio (IR-UWB) is a wireless communication technology well-suited for short range communications (about 10 meters) and has the advantage to allow real-time location with a precision of 5 cm. However, its use has been standardized in some standards and especially in the IEEE 802.15.4 dedicated to Wireless Personnal Area Network (WPAN) and in the IEEE 802.15.6 dedicated to Wireless Body Area Network (WBAN). After presenting requirements of each standard and a literature survey on the IR-UWB emitter, the design of a multi-standard IR-emitter based on the frequency transposition pulse synthesis is proposed in a 28 nm FD-SOI technology. The proposed design has been validated at the transistor level using electrical simulations which take into account the parasitic capacitance at each critical node of the circuit. Moreover, results show that the proposed circuit has the potential to be the first multi-standard IR-UWB emitter which covers every channel of the IEEE 802.15.4 and 802.15.6 standards.**

***Index Terms*— Impulse Radio; Ultra-WideBand; Emitter, Pulse Generator, Multi-standard**

I. Introduction

The Wireless Body Area Networks (WBAN) and Wireless Personal Area Networks (WPAN) are wireless networks well-suited for communications between devices placed near to the human body which require a transmission rate up to 10 Mbps. The WPAN and the WBAN have been respectively standardized by the IEEE 802.15.4 standard (10 m range) and the IEEE 802.15.6 (2 m range), both looking for the optimization of the power consumption according to their own targeted range [1]. Both standards have several applications such as wellness, safety, sports, internet of things and healthcare [2, 3].

Ultra-wideband Impulse Radio (IR-UWB) has been defined as physical (PHY) layer of the WBAN and WPAN standards. On the contrary of narrow-band devices which use a modulated carrier to perform data transmission, standardized IR-UWB devices use short pulses (less than 5 ns and so leading to a large bandwidth) with a central frequency between 3.1 GHz and 10.6 GHz. This short duration allows UWB pulses to have distinguishable multi-path interferences and also to be robust to multipath fading [4], in addition to allow a real time location with an accuracy of 5 cm [5]. Moreover, IR-UWB allows to duty-cycle transceiver power at the bit scale and presents a power consumption proportional to the data rate (on the contrary of narrow-band devices that have a power consumption independent of the data rate) [6]. Thus, a low data rate leads to a low power consumption for IR-UWB devices [7, 8].

IR-UWB communications have been largely studied in literature but the design of a multi-standard IR-UWB transmitter stays an important research topic. Indeed, the WBAN and WPAN IEEE standards introduce different spectral masks to respect. Moreover, the WBAN one defines several different bandwidths for the standardized channels. Since an IR-UWB emitter is a pulse generator, it is also necessary to design pulse generators with envelope shaping and central frequency changing capabilities to obtain a multi-standard design. Moreover, this versatility must be fine enough to compensate Process, Voltage and Temperature (PVT) variations whose pulse generators are very sensitive. Finally, the pulse generator tuning capabilities must allow sidelobes rejection to be high enough to protect adjacent channels. For these reasons, IR-UWB emitters are in fact more pulse synthesizers than pulse generators as it can be seen in literature.

Published IR-UWB emitters compliant with IEEE standards are mainly based on two pulse synthesis method : the direct pulse synthesis and the frequency transposition pulse synthesis. Considering the direct pulse synthesis technique, the pulse is directly generated within the frequency band of interest using an architecture based on delay lines [7, 9]. However, in literature, UWB transmitters based on delay lines seem to be able to generate pulses with a central frequency span no more than 4 GHz, which is not enough to cover all the 3.1 GHz - 10.6 GHz [8], but achieve very high sidelobes rejection.

On the other hand, the frequency transposition pulse synthesis consists in the modulation of oscillations coming from an oscillator using a baseband pulse. The reported architectures are generally based on a mixer and an oscillator (LC-tank or ring oscillator) [10, 11]. To save power, the integrated oscillator must have the capability to be started-up and turned-off as fast as possible in order to minimize the duration between two consecutive pulse transmissions where the oscillator is turned-on [12, 13]. Compared to delay lines architectures, UWB transmitters based on ring oscillators have demonstrate in literature their ability to cover a large central frequency span and also a large number of IEEE 802.15.4 and 802.15.6 channels [14, 15].

In this paper, after introducing IR-UWB signals requirements, a literature survey of IR-UWB emitters with tuning capabilities is done. Next, an IR-UWB transmitter designed to address every channel of the IEEE 802.15.4 and 802.15.6 standards is proposed and validated using simulations. It is

Digital Object Identifier 10.29292/jics.v18i3.793

based on a fast start-up ring oscillator, and a sample and hold envelope shaping circuit which acts as a mixer and an antenna driver. The use of a sample and hold envelope instead of an analog one has been chosen here to make simpler the circuitry required to control pulses shape in addition to allow an envelope tuning fine enough to compensate PVT variations and keep high enough sidelobes rejection.

This article is organized as follows. Section II introduces IR-UWB signals requirements from regulations and IEEE standards point of view. Moreover, it provides an analytical model of pulse in addition to details some examples of pulses envelopes whose a sample and hold one. Next, section III presents a literature survey of UWB transmitters based on the direct and the frequency transposition pulse synthesis addressing several standardized IEEE channels. A multi-standard IR-UWB transmitter using a FD-SOI 28 nm technology is also proposed in section IV. Section V provides simulations results at the transistor level to validate the design. In a first time, parametric simulations are presented to show the tuning capabilities of the proposed pulse generator and in a second time, pulses addressing several IEEE 802.15.4 and IEEE 802.15.6 channels are shown. Finally, section VI concludes the paper.

II. IR-UWB Signals Requirements

A. Regulations and Standards Requirements

FCC has defined the frequency band between 3.1 GHz and 10.6 GHz as the UWB frequency band in 2002 [16]. This frequency band can be used only by an UWB signal. According to FCC, an UWB signal must have its central frequency f_c inside the UWB frequency band. In addition, it must have either a minimal absolute bandwidth BW of 500 MHz or a minimal fractional bandwidth B_{frac} of 20%, for an attenuation X of 10 dB. The fractional bandwidth can be expressed as follows:

$$B_{frac} = \frac{BW_{-XdB}}{f_c}. \quad (1)$$

According to FCC regulations, an UWB signal can have a maximum effective isotropic radiated power density (EIRP) of -41.3 dBm/MHz and a maximum radiated peak power, around the central frequency of 0 dBm. Finally, FCC defines two frequency masks, one for indoor applications and a more restrictive one for outdoor applications shown in Fig. 1.

On the other hand, the European Telecommunications Standards Institute (ETSI) authorizes nowadays the use of UWB communications only in the 6 GHz - 8.5 GHz frequency band, with a maximum EIRP of -41.3 dBm/MHz [17]. Nevertheless, ETSI has initially authorized UWB communications inside the 3.1 GHz - 4.9 GHz frequency band too.

Figure 1 shows the maximum mean power spectral density (PSD) of an UWB signal as defined by FCC for both indoor and outdoor applications, in addition to the one defined by ETSI. Next, several UWB frequency bands have been defined all around the world, generally similar to FCC or ETSI ones. To make uniform the use of the UWB frequency band in each country or world region and also to enable the design of UWB transceivers working all around the world, some

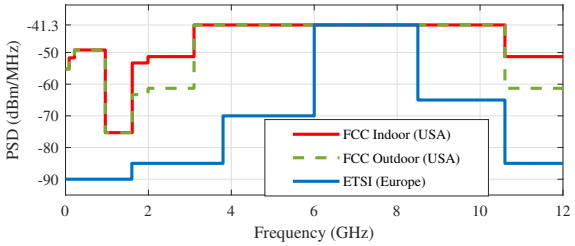

Fig. 1 FCC and ETSI spectral masks.

standards have been defined and especially two IEEE ones : the IEEE 802.15.4 standard and the IEEE 802.15.6 standard. The both introduce their own set of channels, these last being defined by their central frequency, their bandwidth, and their radio-frequency masks.

The IEEE 802.15.4 standard, introduced in 2011, is dedicated to low power WPAN applications [18]. This IEEE standard defines 16 channels, each one associated to one of the 3 groups defined in this standard: the sub-GHz group, the low band group and the high band group. It can noticed that 12 on 16 channels have a bandwidth of 500 MHz. In addition, the only one channel inside the sub-GHz group is not considered in this paper since it is not inside the UWB frequency band defined by FCC (3.1 GHz to 10.6 GHz).

The IEEE 802.15.6 standard, introduced in 2012, targets WBAN applications [19]. This IEEE standard defines 11 channels, each one associated to one of the 2 groups defined in this standard: the low band group and the high band one. It can be noticed that every channel has a 500 MHz bandwidth.

Figures 2 and 3 displays the channels frequency plan of these IEEE standards. In terms of sidelobes rejection, the IEEE 802.15.4 (resp. 802.15.6) standard has established a minimal level of 18 dB (resp. 20 dB) as shown in Figure 4 where the IEEE 802.15.4 and 802.15.6 standardized spectral masks of 500 MHz channels can be seen. From the designer point of view, the main issues are here to cover each standardized channel between 3.1 GHz and 10.6 GHz, while having a sidelobes rejection high enough to protect adjacent channels. While the first issue is more a design issue, the sidelobes rejection issue is more a fundamental issue that requires to investigate the UWB pulse envelope, which can have an impact on the UWB emitter architecture itself.

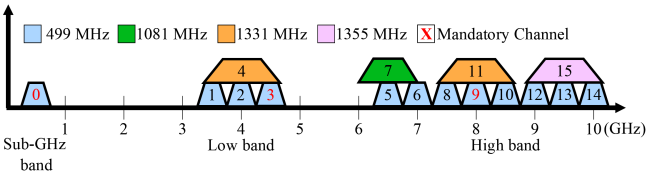

Fig. 2 IEEE 802.15.4 standard channels frequency plan.

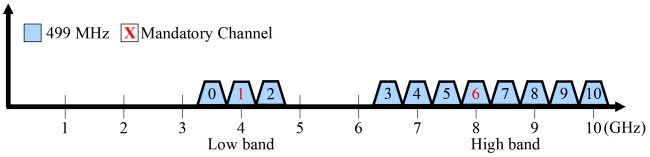

Fig. 3 IEEE 802.15.6 standard channels frequency plan.

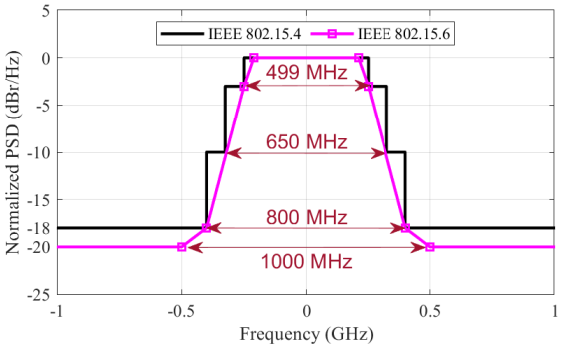

Fig. 4 IEEE standards spectral mask (BW_{-3dB} = 499 MHz).

B. *UWB Pulses Envelope Characteristics*

An UWB pulse can be described as a modulated sine-wave as follows:

$$p(t) = x(t) \cdot \cos(2\pi f_m t - \phi) \tag{2}$$

where $x(t)$ is the pulse envelope, f_m the frequency for which the pulse power spectral density reaches its maximum value, and ϕ the sine-wave phase. The mono-lateral Fourier transform of this pulse can be expressed as follows:

$$P^{+}(f) = \frac{1}{\sqrt{2}} \cdot X(f - f_m) \cdot e^{-j\phi} \tag{3}$$

where $X(f)$ is the envelope Fourier transform. However, since the UWB signal PSD is directly proportional to the Fourier transform magnitude of the emitted pulses [20], it is possible to conclude that the UWB signal PSD shape is given by the Fourier transform magnitude of the pulses envelope. Thus, the pulse envelope must be chosen according the targeted spectral mask.

In this part, three types of envelopes shapes are detailed: the rectangular, the triangular, and the sample and hold envelope.

The rectangular envelope, the simplest one, can be written as follows:

$$x_R(t) = A \cdot \Pi_{\tau_P}(t) \tag{4}$$

where $\Pi(t)$ is the gate function and A (resp. τ_P) is the envelope amplitude (resp. width). This envelope also performs a rectangular windowing over the sinusoidal waveform. Shifting to frequency domain, the rectangular envelope Fourier transform can be computed as:

$$X_R(f) = A \cdot \tau_P \cdot \text{sinc}(\pi f \tau_P) \tag{5}$$

Finally, the energy associated to one rectangular pulse can be written as follows:

$$E_{P-R} = \frac{A^2 \tau_P}{2Z_L} \tag{6}$$

where Z_L is the considered impedance load. Figure 5 presents a rectangular pulse in time and frequency domain, addressing both channel 3 of the IEEE 802.15.4 standard and channel 2 of the IEEE 802.15.6 standard. However, it is possible to see on this figure that the rectangular pulse does not satisfy the minimum 10 dB bandwidth of 500 MHz imposed by FCC while it respects the IEEE sidelobes rejection. To be compliant with the FCC minimum bandwidth, the rectangular should be shorter but in this case, the sidelobes having a rejection of about 13.5 dB will move to adjacent channels. Therefore, the rectangular envelope do not allow the spectral requirements imposed by both FCC regulations and IEEE standards to be respected simultaneously.

The triangular envelope can be expressed as follows:

$$x_T(t) = \begin{cases} A\left(1 - \frac{2|t|}{\tau_P}\right) & if \quad 0 < |t| < \frac{\tau_P}{2} \\ 0 & otherwise \end{cases} \tag{7}$$

and its Fourier transform is given by:

$$X_T(f) = A \cdot \tau_P \cdot \text{sinc}^2(\pi f \tau_P) \tag{8}$$

Finally, the energy associated to a triangular pulse is given as follows:

$$E_{P-T} = \frac{A^2 \tau_P}{8Z_L} \tag{9}$$

Figure 6 shows a triangular pulse in time and frequency domain, addressing both channel 3 of the IEEE 802.15.4 standard and channel 2 of the IEEE 802.15.6 standard. Compared to the rectangular pulse, the triangular pulse can have the required sidelobes rejection level (27 dB versus 18 or 20 dB required) while having a 10 dB bandwidth greater than 500 MHz. Thus, a triangular envelope allow FCC and IEEE requirements to be respected simultaneously. Nevertheless, this envelope is not easy to generate from the electronic point of view. However, it can be noted that other pulse envelopes allow high sidelobes rejection level such as the Gaussian one [21] or the cardinal sine one.

To simplify the generation of triangular or similar envelopes, it is proposed to approximate an analog envelop such as the presented triangular one by a sample and hold envelope. In the general case, the sample and hold envelope can be represented as a combination of rectangular time shifted functions, with different amplitudes which can be expressed as follows:

$$x_{SH}(t) = \sum_{k=0}^{K-1} x_C(k \cdot \tau_S - \alpha) \cdot \Pi_{\tau_S}(t - k \cdot \tau_S + \alpha) \tag{10}$$

with:

$$\alpha = \tau_S \frac{K-1}{2} \tag{11}$$

and where τ_e is the sample time, K the number of samples and $x_c(t)$, the considered analog envelope (such as the triangular one). The Fourier transform of this envelope can be written as follows:

$$X_{SH}(f) = e^{-j\pi f \alpha} \cdot \text{sinc}(\pi f \tau_S) \sum_{k=0}^{K-1} X_C\left(f - \frac{k}{\tau_S}\right) \tag{12}$$

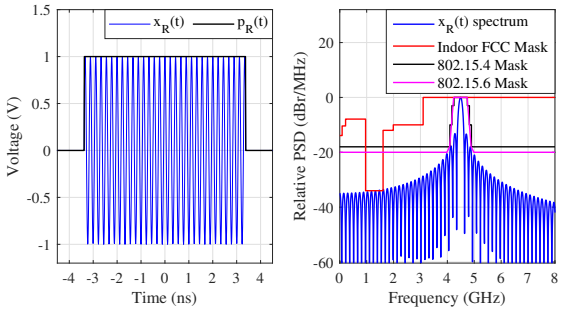

Fig. 5: IR-UWB pulse with rectangular envelope compliant with the channel 3 of IEEE 802.15.4 standard and channel 2 of IEEE 802.15.6 (BW_{-3dB} = 499 MHz and τ_p = 6.75 ns).

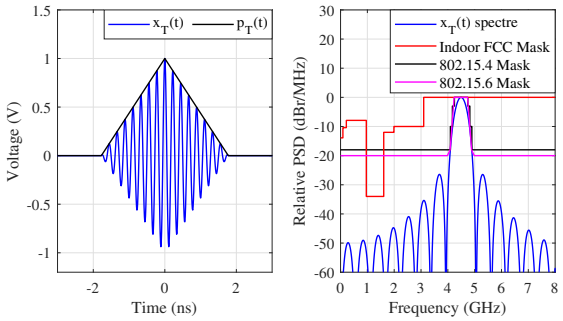

Fig. 6: IR-UWB pulse with triangular envelope compliant with channel 3 of the IEEE 802.15.4 standard and channel 2 of the IEEE 802.15.6 (BW_{-3dB} = 499 MHz and τ_p = 3.55 ns).

Finally, the energy associated to this sample and hold pulse can be written as follows:

$$E_{P-SH} = \frac{\tau_p}{2 \cdot Z_L} \sum_{k=0}^{K-1} x_C^2 \left(k \cdot \tau_S - \alpha\right) \tag{13}$$

Figure 7 shows a sample and hold triangular pulse in time and frequency domain, addressing both channel 3 of IEEE 802.15.4 standard and channel 2 of IEEE 802.15.6. It is also possible to notice that the sample and hold triangular pulse has a lower sidelobes rejection compared to the triangular one. Nevertheless its sidelobes rejection can be enough regarding the one imposed by IEEE standards for adjacent channels. However, it can be noticed that with this pulse, the FCC mask is not fully respected between 1 GHz and 2 GHz. But, this is not an issue since the antenna should be designed to meet the FCC spectral requirements outside the targeted frequency bands. Finally, Table I shows the characteristics of all sample and hold triangular envelopes which are necessary to comply spectral requirements of all IEEE 802.15.4 and 802.15.6 channels.

III. IR-UWB TRANSMITTERS LITERATURE SURVEY

As indicated previously, IR-UWB emitters are generally pulse synthesizers (which allow to control pulses envelope compared to pulse generators) in literature and two main pulse synthesis methods are reported: the pulse direct synthesis and the frequency transposition pulse synthesis.

Considering the first method, the pulse is directly synthesized within the targeted frequency band using a delay line

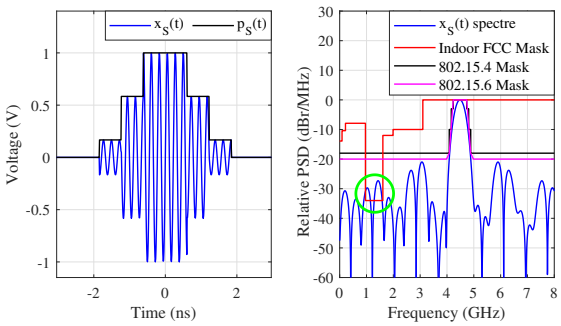

Fig. 7: Example of IR-UWB pulse with sampled & hold envelope compliant with the channel 3 of IEEE 802.15.4 standard and channel 2 of IEEE 802.15.6 (BW_{-3dB} = 499 MHz and τ_p = 3.55 ns).

such as a voltage control delay line (VCDL). Considering the second method, the pulse is a baseband pulse transposed to the targeted frequency by modulating oscillations coming from an oscillator such as a voltage-controlled oscillator (VCO) whose architecture can be based on a LC-tank or a ring oscillator.

A. *IR-UWB Emitters based on Direct Pulse Synthesis*

The direct pulse synthesis is performed with a circuit composed of delay cells. The IR-UWB pulse is generated directly in the targeted frequency band using voltage-controlled delay cells (baseband pulse generator) and a edge combiner (baseband pulse combiner) as shown in [1]. Thus, a set of delay cells, tuned by voltages, generates time shifted baseband pulses which are combined in a edge combiner circuit. However, narrower the targeted channel is and higher the central frequency is, higher the required number of delay cells is. For this reason, this pulse synthesis method is mainly used when a frequency band greater than 1 GHz with a central frequency less than 5 GHz are targeted such as in [1] where the 3.1 GHz - 4.9 GHz frequency band is targeted.

However, an IR-UWB transmitter front-end in 65 nm bulk CMOS technology for energy-harvesting devices, with pulse shaping capabilities and integrated output matching network, is reported in [8]. This IR-UWB transmitter is able to generate pulses having a central frequency between 6 GHz and 8.5 GHz. Its architecture is displayed in Figure 9 and requires lots of delay cells as expected (32 delay cells). The main blocks of this transmitter are delay cells (δ), routers (R), combiners (C), a power amplifier (PA) and a matching network (MN). The delay line, composed by 32 delay cells, generates a pulse whose the central frequency is controlled by the propagation delay. This delay is digitally controlled using a 9-bit word and each delay cell generates an impulse at router input. Next, the routers propagate the input pulse to up to 4 parallel outputs based on a 4-bit tuning word. The generated signal from routers are then combined into the combiners, and finally the combined pulses are sent to the PA and the matching network. The main advantage of this architecture is that it requires only one PA instead of 32 sub-PAs. However, addressing high pulse central frequencies implies a larger number of delay cells as explained earlier, which increases the complexity of the pulse combiner circuit layout due to larger parasitic capacitances, and also

Table I. Sample and hold triangular envelope characteristics for the generation of UWB pulses compliant with the IEEE 802.15.4 and 802.15.6 standards

Standard	Associated channel	BW_{-3dB} (MHz)	Minimal sidelobes Rejection (dB)	τ_S (ps)	Number of Samples	τ_P (ps)	Sampling Frequency (GHz)
IEEE 802.15.4	0, 1, 2, 3, 4, 5, 6, 8, 9, 10, 12, 13 and 14	499	18	626	6	3756	1.60
IEEE 802.15.4	7	1081	18	235	6	1404	3.37
IEEE 802.15.4	4 and 11	1331	18	297	6	1410	4.27
IEEE 802.15.4	15	1355	18	231	6	1386	4.33
IEEE 802.15.6	0 to 11	499	20	626	6	3756	1.60

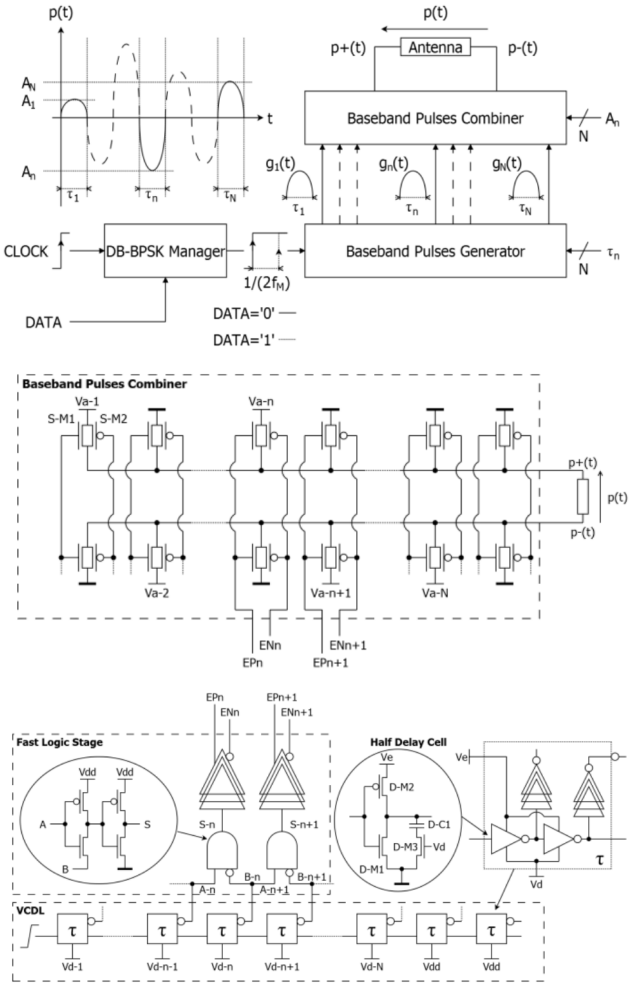

Fig. 8 Example of an IR-UWB emitter based on direct pulse synthesis [1].

impacts the central frequency range itself. Nevertheless, this transmitter presents a high sidelobes rejection (30 dB) and it is able to generate pulses with a larger bandwidth, such as the channel 8 of the IEEE 802.15.4 standard.

B. IR-UWB Emitters based on frequency transposition pulse synthesis

The pulse synthesis method based on frequency transposition requires a local oscillator. This oscillator has to generate oscillations with the targeted central frequency and these oscillations must be modulated by a baseband pulse whose the envelope depends on the targeted spectral mask. Thus, this synthesis technique requires a pulse shaping circuit able to apply on the oscillations an envelope compliant with FCC and IEEE standards requirements. However, to address with the same circuit 499 MHz bandwidth or higher ones as expected for channels 4, 7, 11 and 15 of the IEEE 802.15.4, the bandwidth of the mixing circuit shall be very large which generally increases the circuit complexity and the power consumption.

To avoid the use of a mixing circuit, a reported strategy consists in modulating the VCO through its supply voltage, leading to the so-called gated VCO. The oscillator settling time and the extinction time, in addition to the start and stop signal shape, are then critical to cover channels which require pulses having a duration of some nanoseconds.

In [11], a gated VCO shown in Fig. 10 is used to design an IR-UWB transmitter front-end which is powered by a radio frequency energy harvester. It has been design in a 180 nm CMOS technology and targets ETSI compliant frequency masks (channels between 6 GHz and 8.5 GHz). The transmitter architecture is based on a duty-cycled cross-couple-pair LC oscillator (oscillator core), that generates a single pulse for every rising edge at Vtrig node. This architecture allows the pulses bandwidth, the central frequency, and the amplitude to be tuned according to the targeted channel and to compensate PVT variations. About the center frequency, it can be tuned between 5.98 GHz and 8.80 GHz using a 6-bit capacitors bank (C). The pulse duration, and also the pulse bandwidth, is controlled by the delay stage which generates from the input signal V_{TRIG} two delayed control signals for the n-channel transistors M3 and M4. This delay and also the pulse duration is then controlled by a 6-bit capacitors bank (C_{BW}). The pulse magnitude is controlled in the output stage using a programmable current source (bottom part) with a 4 bits gain control word. Finally, an external output-balun is driven by a matching circuit controlled by a 6-bit bank capacitor (C_{MP}). This transmitter presents an output amplitude of 1.0 Vpp which is greater than [8], and has a low energy consumption (6.2 pJ per bit for a data rate of 0.11 Mbps). In addition, even if this transmitter has a central frequency range larger than [8], it is not wide enough to cover all the FCC band. Besides, unlike [8], the transmitter described in [11] cannot generate pulses having a bandwidth greater than 1 GHz.

The use of ring oscillators, that are capable of fast start-up and turned-off, allowing the generation of ultra-short pulses (less than 1 ns) with a good output voltage dynamic, has been equally reported for the design of IR-UWB emitter in [12] where a voltage controlled ring oscillator requiring only MOS transistors is proposed.

In [22], the use of a ring oscillator is equally considered to design an IR-UWB transmitter using a 28 nm FD-SOI CMOS technology allowing channel selection and digitally programmable pulse shaping. Figure 11 shows the proposed architecture which exploits the forward back biasing

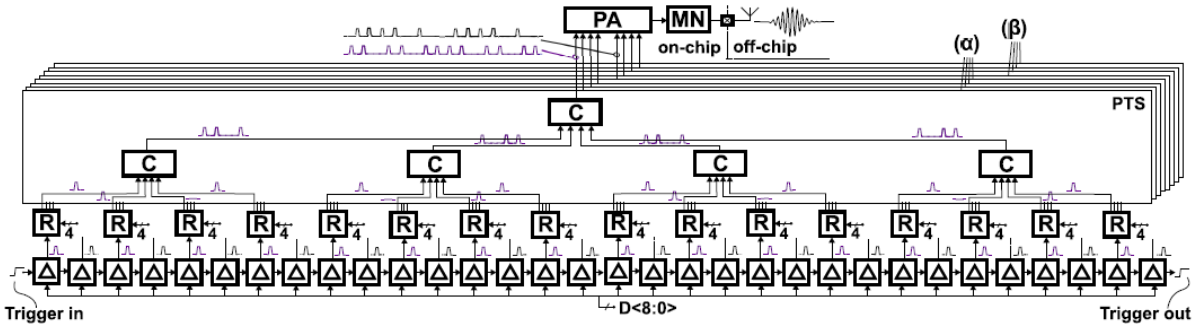

Fig. 9 Delay line-based transmitter front-end architecture [8].

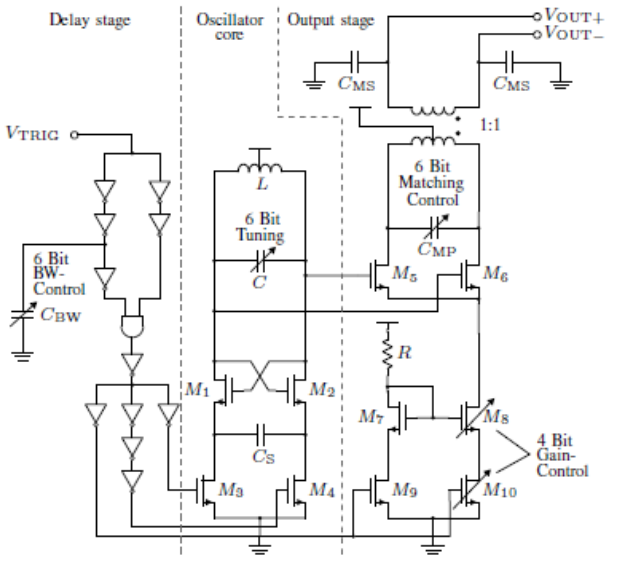

Fig. 10: IR-UWB transmitter architecture based on cross-couple-pair LC oscillator [11].

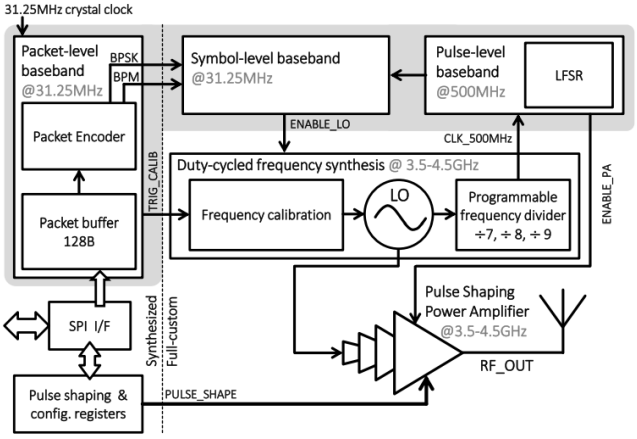

Fig. 11 Transmitter architecture based on controlled ring oscillator [22].

(through the MOS back gate which is a specificity of FD-SOI technologies) to reduce the MOS transistor threshold voltage, compensate PVT variations, and tune the pulse central frequency. The local oscillator used in this work is a 7 stages ring oscillator (Fig. 11) which allows to control the pulse central frequency between 3.5 GHz and 4.5 GHz, which is the lowest central frequency range presented in this survey. Moreover, this transmitter has a sidelobes rejection of 20 dB (lower than [8]), and an energy consumption of 24 pJ per bit for a data rate of 27.24 Mbps.

In [23], an IR-UWB transmitter in 28-nm CMOS technolgy compliant with IEEE 802.15.4z is presented. Its architecture based equally on a ring oscillator is shown in Fig. 12. It can generate UWB pulses with a sample and hold envelope, like the one shown in Fig. 7 but with a variable sample frequency all along the pulse duration. Thus, in this paper, the sample time is tuned through the pulse shaper which includes a digitally programmable delay line. The delay line output signals are then combined to obtain the targeted envelope which is here an approximation of the triangular envelope. This transmitter presents a sidelobes rejection of 29 dB, which is close to the one of [8], but allows a central frequency between 3 GHz and 10 GHz which is the largest central frequency range in the literature. However, this transmitter cannot generate a pulse with a 3 dB bandwidth larger than 1 GHz as required by channels 4, 7, 11 and 15 of the IEEE 802.15.4 standard. In terms of energy consumption, the transmitter of [23] has an energy consumption of 180 pJ per bit for a data rate of 27.24 Mbps.

In table II, a qualitative comparison between the presented IR-UWB emitters is done. It appears that the transmitter presented in [23] is the best in terms of central frequency range, despite it has the highest energy consumption. More generally, the transmitters based on ring oscillators are the most interesting regarding the pulse central frequency range. Meanwhile, the transmitter of [8] is the best in terms of bandwidth tuning range, being potentially able to generate signals with a 3 dB bandwidth between 500 MHz and 1355 MHz. Finally, [23] and [8] are able to provide a sidelobes rejection better that the ones required by the IEEE standards. Thus, emitters based on frequency transposition pulse synthesis can achieve similar sidelobes rejection than the ones based on direct pulse synthesis with a sample and hold en-

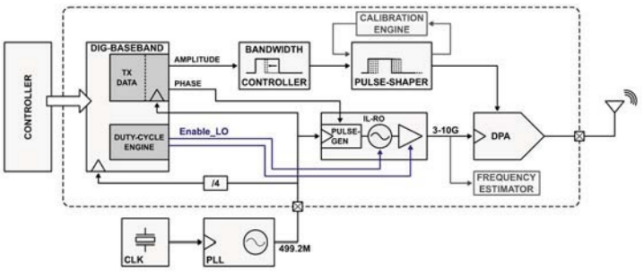

Fig. 12: IR-UWB Transmitter comply with IEEE 802.15.4z architecture [23].

Table II. Performance Comparison.

	JSSC'20 [8]	ITCS'20 [11]	JSSC'17 [22]	ISSCC'21 [23]
Architecture	Delay-line based	LC oscillator based	Ring oscillator based	Ring oscillator based
Oscillation frequency tuning range	-	-	- -	+
sidelobes rejection	++	+	+	++
BW_{-3dB} tuning range	++	-	-	- -
Output voltage level	+	++	++	- -
Energy per pulse consumption	-	++	++	- -

++ : very good, + : good, - : bad, - - : very bad

velope if the sample time is not constant. However, emitters based on frequency transposition pulse synthesis do not demonstrate yet their ability to generate pulses with a sufficient bandwidth tuning range to cover the all requirements of the IEEE 802.15.4 standard in terms of bandwidth.

IV. Design of a Multi-Standard IR-UWB Transmitter

From the literature survey, an IR-UWB transmitter based on frequency transposition pulse synthesis seems to be the best choice to address every IEEE 802.15.4 and 802.15.6 channels. Nevertheless, the required local oscillator must cover the frequency band between 3.1 GHz and 10.6 GHz while being able to fast start-up and turned-off to minimize the power consumption when no pulse is generated. Indeed, it is necessary to generate short pulses of a few ns to fit into IEEE spectral masks and a ring oscillator should be a relevant choice. Finally, to make easy the control of the pulse envelope while having a sidelobes rejection high enough to meet IEEE standards requirements, the use of a sample and hold envelope seems to be a good choice from the presented theoretical analysis and the literature review. For these reasons, it is proposed here to design a multi-standard IR-UWB transmitter based on the frequency transposition pulse synthesis using a sample and hold envelope and implementing a ring oscillator.

The proposed IR-UWB transmitter is also designed to generate pulses compliant with every IEEE standardized channels between 3.1 GHz and 10.6 GHz. Moreover, to properly control the pulse shape and also the emitted spectrum (especially bandwidth and sidelobes rejection), the proposed circuit allows the central frequency in addition to the amplitudes, the number, and the duration of the samples shown in Fig. 13 to be controlled.

The transmitter architecture, which consists in 6 main blocks, is shown in Figure 14. The first block (a) is a VCO with a fast start and stop ability. Moreover, this VCO is able to generate pulse with a central frequency within the entire FCC frequency band (i.e. 3.1 GHz - 10.6 GHz). The second block (b) is an amplifier whose the gain is digitally controlled

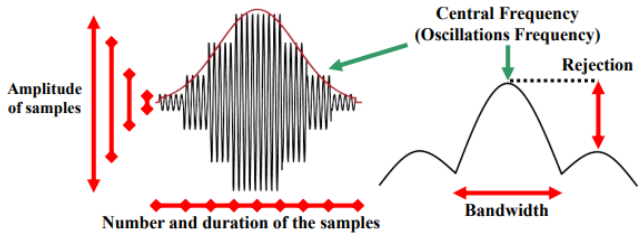

Fig. 13 UWB pulses parameters that can be tuned.

(DCA) in order to modulate the amplitude of the oscillations coming from the oscillator. The third block (c) is a buffer circuit which must guarantee a good transmission of the oscillations from VCO to the DCA. The fourth block (d) is a digital envelope generator. It is in charge of the data generation for controlling the DCA gain in order to obtain on the DCA outputs a pulse having the desired sample and hold envelope. Considering how fast these data should be transmitted, the digital envelope generator uses a fast memory (e) based on shift registers which are refreshed before every pulse generation using a parallel loading from a slow memory (e) whose the role is to permanently store the data to transmit. The sixth block (f) is a double band digitally controlled oscillator (DB-DCO). The DB-DCO generates the clock, required by the fast memory (d), whose the frequency is directly equal to the reverse of the envelope samples duration. Finally, it can be noted that every block presented here can be turned-off to minimize the power consumption when no pulse is generated.

To cover entirely the targeted frequency band, Current Mode Logic (CML) logic has been used to implement the blocks (a), (b) and (c). It is important to note that the DCA gain and the DB-DCO oscillations frequency are controlled each one by a 8-bit word, in order to allow a fine tuning of the samples amplitude (DCA) and the samples duration (DB-DCO). It must be noted that this tuning is fine enough to compensate PVT variations. Moreover, the DB-DCO has an additional bit to select the samples duration range (between 220 ps and 330 ps or between 0.5 ns and 1 ns, which is enough for the targeted sample and hold triangular pulse to cover every IEEE channels as shown in Table I).

The VCO (a), which generates oscillations having a frequency equals to the targeted central frequency, is based on a ring oscillator architecture as indicated in Figure 15 whose principle is to propagate a signal on a closed loop chain of an odd number of inverters. NAND gates have been implemented instead of inverters, allowing to have a fast oscillations start and stop, in addition to require the design of only one delays cell since NAND gates can act as an inverter if one of the two inputs are set to Vdd. Furthermore, a buffer cell based on a XOR gate allows a 180° phase-shift of the emitted pulse as needed to implement the Binary Phase Shift Keying (BPSK) impulse modulation used for example in the 802.15.4 standard.

The DCA (b) architecture is shown in Fig. 16. Its gain is controlled by the 8 bits word PDB(7:0). Thus, the DCA is able to perform a 256 Amplitude Shift Keying (ASK) modulation on the input oscillations (IN). To approach a linear control of the output oscillations magnitude (OUT), the width of M5 to M12 transistors follows a geometric progres-

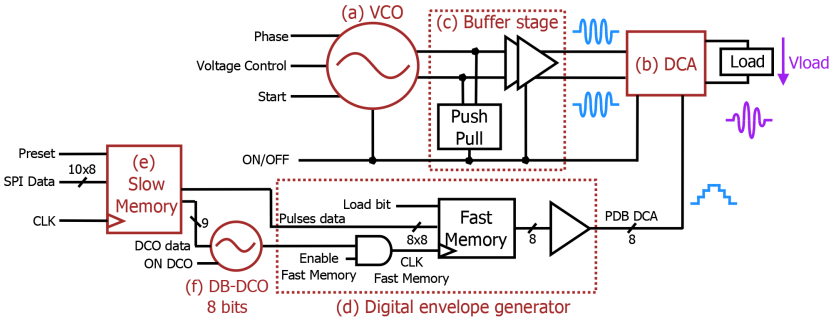

Fig. 14 Proposed UWB transmitter architecture.

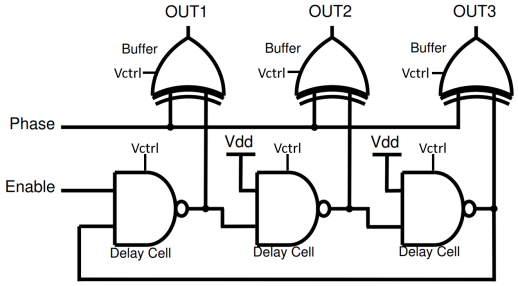

Fig. 15 Voltage controlled ring oscillator topology.

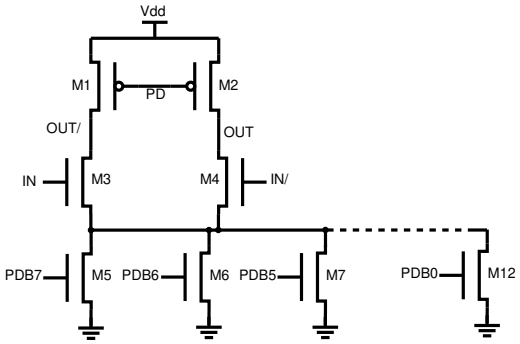

Fig. 16 8-bit DCA transistor level schematic.

sion with a common ratio of 0.5, PDB7 being the Most Significant Bit (MSB) and PDB0 the Less Significant Bit (LSB).

The digital envelope generator (d), which controls the DCA gain during the pulse generation to shape its envelope, contains 8 shift registers as described earlier (1 shift register by PDBx). The architecture of one shift register is shown in Fig. 17. It is composed of 8 D flip-flops (the "Fast Memory"), 1 buffer, 8 NAND gates and 8 inverters. Since a shift register is a First In First Out (FIFO) memory and considering the n^{th} shift register, the bit number n of the first envelope sample is loaded in the last D flip-flop and the bit number n of the last envelope sample is loaded in the first D flip-flop. Figure 18 shows the chronograms related to the digital envelope generator where "D0" to "D7" correspond to the 8 samples magnitudes represented on 8 bits. When no pulse is transmitted, the 8-bit word has a null value. As shown in Fig. 14, an AND gate, placed before the fast memory and enables the fast memory clock. Finally, the signal "Load Bit" allow to initialize the fast memory with the data stored in the slow memory.

Thus, the "Fast Memory" inside the digital envelope generator (d) provides the 8-bit word "PDB DCA" which controls the DCA (b) gain during the pulse generation and so the samples levels. Since the fast memory is a 8×8 bits memory, it enables the generation of pulses having a sample and hold envelope having 8 samples of 8 bits. Besides, the DB-DCO (f) controls the envelope shape through the oscillation frequency since its oscillation period correspond to the sample period. To summarize and according to Fig. 13, the VCO (a) controls the pulse central frequency, the digital envelope generator (d) controls the amplitude of the samples, and the DB-DCO (f) controls the duration of the samples.

V. Simulations Results of the Proposed Multi-Standard IR-UWB Transmitter

This section presents schematic level simulation results of the proposed multi-standard IR-UWB transmitter. The circuit has been implemented using the FD-SOI 28 nm CMOS design kit from STMicroeletronics, with a supply voltage of 1 V. To achieve more realistic and reliable simulations, parasitic capacitances due to layout have been estimated and added at each critical node. Simulation results presented in this part have also been done with these parasitic capacitances. They deal in a first time with tuning capabilities of

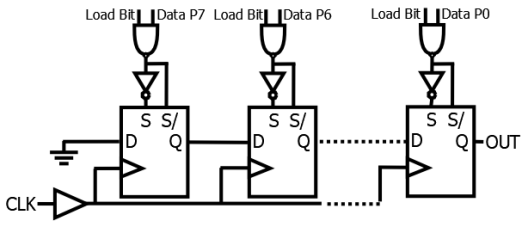

Fig. 17 CMOS Shift Register architecture.

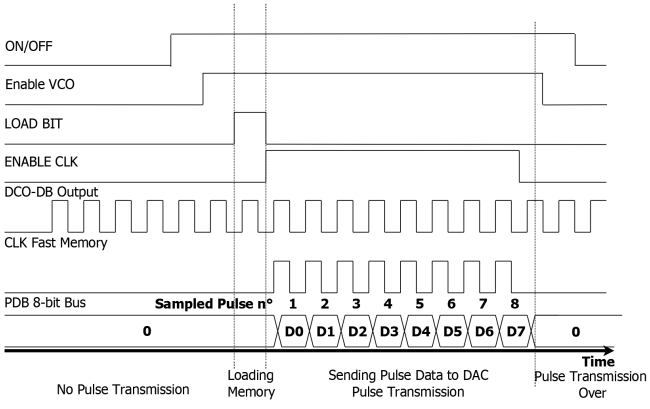

Fig. 18 Chronograms of the envelope shaping circuit.

the pulse generator and in a second time, show several pulses examples compliant with IEEE channels.

A. *Tuning capabilities of the proposed pulse generator*

The VCO frequency and its always-on power consumption as a function of the VCO input control voltage ("Vctrl") are shown in Fig. 19. It is possible to notice that the proposed VCO is able to cover all the 3.1 GHz - 10.6 GHz frequency band as required since its maximum (resp. minimum) oscillations frequency is 13.2 GHz (resp. 1.05 GHz). The always-on power consumption of the VCO which is associated to this frequency is 20.2 mW and is also about 1.53 mW/GHz for the entire frequency band. Finally, the average (resp. minimum and maximum) VCO gain is around -18.1 GHz/V (resp. -20.8 GHz/V and -10.6 GHz/V).

The DCA maximum output amplitude as a function of the VCO frequency is given in Fig. 21, and as a function of the 8-bit word "PDB" in Fig. 22 for the minimum and the maximum channel central frequencies. It can be observed that the DCA maximum amplitude is around 1 Vpp within all the targeted frequency band. Thus, the proposed pulse generator is potentially able to address every IEEE channel. Moreover, it can be seen that the DCA output magnitude is piecewise quasi-linearly controlled by the PDB word. Finally, the always-on power consumption of the blocks (a) to (c) is given in Figure 21.

B. *Pulses generation for several IEEE channels*

Figures 20 and 23 shows IR-UWB pulses addressing IEEE 802.15.4 (resp. IEEE 802.15.6) channels 1 (resp. 0) and 14 (resp. 10) in time and frequency domains. In addition, an IR-UWB pulse addressing the IEEE 802.15.4 channel 15 is shown in Fig. 24. Table I shows the generated IR-UWB pulse parameters for every addressed channel.

It can be noticed from Fig. 20, Fig. 23, and Fig. 24 that generated pulses can respect the spectral masks established by both IEEE 802.15.4 and 802.15.6 standards. However, they do not fit entirely the FCC indoor masks, mostly in the 0.5 GHz - 2.0 GHz frequency band. Nevertheless, this is not a major concern since the UWB antenna should filter this out of FCC frequency band spectrum part.

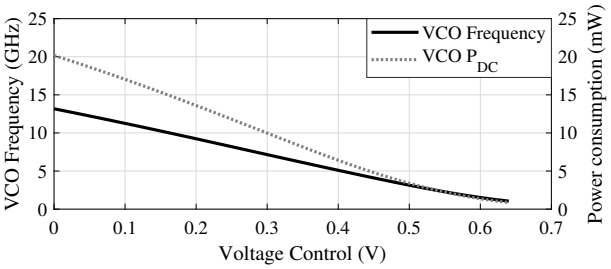

Fig. 19: VCO frequency and always-on power consumption in terms of VCO voltage control.

Table III. Parameters associated to simulated IR-UWB pulses

IEEE 802.15.4 Channel	1	14	15
IEEE 802.15.6 Channel	0	10	-
VCO Voltage Control (mV)	500	192	216
Central Frequency (MHz)	3494	9984	9484
BW_{-3dB} (MHz)	499	499	1355
Envelope sampling frequency (GHz)	1.40	1.54	3.91
Sampled pulse duration (ps)	716	651	256
Pulse total duration (ps)	4296	3906	1536

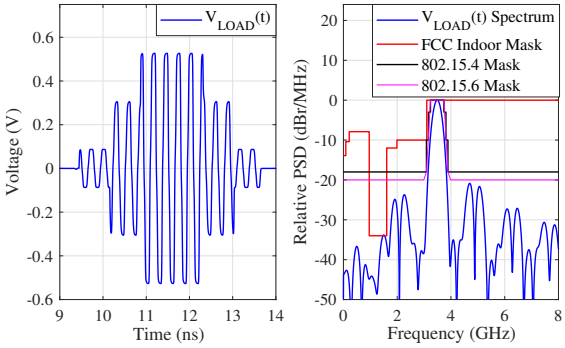

Fig. 20: IR-UWB pulse for the channel 1 of the IEEE 802.15.4 standard (channel 0 of IEEE 802.15.6 standard).

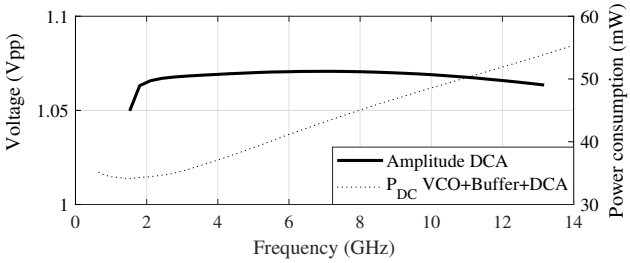

Fig. 21: DCA output voltage and always-on power consumption as a function of the VCO frequency.

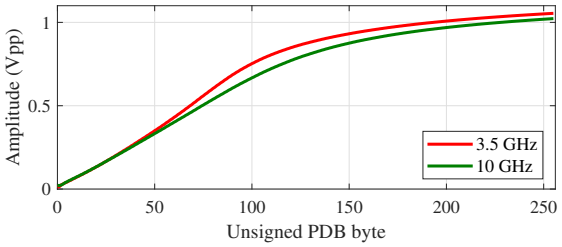

Fig. 22 DCA output voltage as a function of the 8-bit word "PDB".

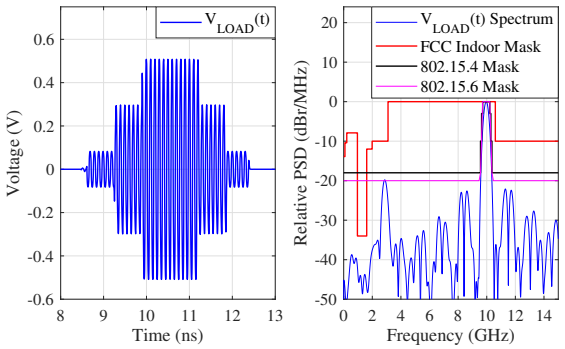

Fig. 23: IR-UWB pulse for the channel 14 of the IEEE 802.15.4 standard (channel 10 of IEEE 802.15.6 standard).

As indicated earlier, the power consumption of an IR-UWB pulse generator is proportional to the pulse rate and also can be written as as follows:

$$P_c = E_{AC} \cdot PRF + P_{0Hz} \tag{14}$$

where E_{AC} is the energy consumption per pulse, PRF the mean pulse repetition frequency, and P_{0Hz} the DC power

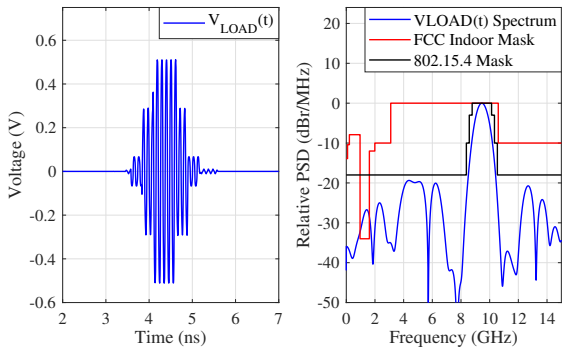

Fig. 24 IR-UWB pulse for the channel 15 of the IEEE 802.15.4 standard.

consumed when no pulse is generated . Assuming these definitions, the presented pulse synthesizer has a P_{0Hz} of 14.53 μW and an E_{AC} of 203.6 pJ/pulse for channel 1 (Fig. 20), 308.3 pJ/pulse for channel 14 (Fig. 23), and 157.7 pJ/pulse for channel 15 (Fig. 24).

Table II presents a comparison between the proposed pulse generator with the state-of-the-art. Compared to the other works, this IR-UWB emitter is the only one that covers the 3.1 GHz - 10.6 GHz and addresses every IEEE 802.15.4 and 802.15.6 channels, which explains the high power consumption but validates the choice of the 28 nm CMOS technology. Finally, the sidelobes rejection is enough to be compliant with IEEE standards but could be improved at the state-of-the-art if a variable sample frequency is used instead of a fixed one. From our knowledge, no figure of merit has been defined to fairly compare UWB transmitters. The UWB transmitters must also be compared regarding their different characteristics.

VI. Conclusion

In this paper, IR-UWB signals requirements from regulations and IEEE standards point of view have been given. In addition, an analytical model of pulse has been provided and some examples of pulses envelopes have been detailed whose the sample and hold one. Next, a literature review of some UWB transmitters, based on direct pulse synthesis and frequency transposition pulse synthesis, has been done and shows that a multi-standard IR-UWB shall be based on the frequency transposition method. Following that, the architecture of a multi-standard IR-UWB emitter based on the frequency transposition pulse synthesis is proposed and fully described. Finally, schematic simulations results taking account layout parasitic capacitances at each critical node are provided and demonstrate ability of the proposed IR-UWB transmitter to cover every IEEE channel.

References

[1] R. Vauche, E. Muhr, O. Fourquin, S. Bourdel, J. Gaubert, N. Dehaese, S. Meillere, H. Barthelemy, and L. Ouvry, "A 100 MHz PRF IR-UWB CMOS transceiver with pulse shaping capabilities and peak voltage detector," *IEEE Transactions on Circuits and Systems I: Regular Papers*, vol. 64, no. 6, pp. 1612–1625, June 2017.

[2] J. Wang and Q. Wang, *Body Area Communications: Channel Modeling, Communication Systems, and EMC*, 1st ed. Piscataway, NJ, USA: IEEE Press, 2013.

[3] J. Kim, J. Choi, and K. Kim, "Robust detection of presence of individuals in an indoor environment using ir-uwb radar," *IEEE Access*, vol. 8, pp. 108 133–108 147, 2020.

[4] D. Dardari, A. Conti, U. Ferner, A. Giorgetti, and M. Z. Win, "Ranging with ultrawide bandwidth signals in multipath environments," *Proceedings of the IEEE*, vol. 97, no. 2, pp. 404–426, 2009.

[5] A. Goavec, M. Zarudniev, R. Vauché, F. Hameau, J. Gaubert, and E. Mercier, "An efficient method of power spectral density estimation for on-chip IR-UWB transmitter self-calibration," *IEEE Transactions on Circuits and Systems I: Regular Papers*, vol. 64, no. 3, pp. 686–695, March 2017.

[6] R. Vauche, S. Bourdel, N. Dehaese, J. Gaubert, O. Ramos Sparrow, E. Muhr, and H. Barthelemy, "High efficiency uwb pulse generator for ultra-low-power applications," *International Journal of Microwave and Wireless Technologies*, vol. 8, no. 3, p. 495–503, 2016.

[7] T. Haapala, M. Pulkkinen, J. Salomaa, and K. Halonen, "A 180-nW static power UWB IR transmitter front-end for energy harvesting applications," in *2017 IEEE International Symposium on Circuits and Systems (ISCAS)*, May 2017, pp. 1–4.

[8] T. Haapala, T. Rantataro, and K. A. I. Halonen, "A fully integrated programmable 6.0–8.5-ghz uwb ir transmitter front-end for energy-harvesting devices," *IEEE Journal of Solid-State Circuits*, vol. 55, no. 7, pp. 1922–1934, 2020.

[9] R. Vauché, S. Bourdel, E. Muhr, J. Gaubert, N. Dehaese, F. Hameau, and H. Barthelemy, "Design of pulse synthesizers for the convergence of ir-uwb solutions," in *2016 14th IEEE International New Circuits and Systems Conference (NEWCAS)*, 2016, pp. 1–4.

[10] R. Dokania, X. Wang, S. Tallur, C. Dorta-Quinones, and A. Apsel, "An ultralow-power dual-band uwb impulse radio," *IEEE Transactions on Circuits and Systems II: Express Briefs*, vol. 57, no. 7, pp. 541–545, 2010.

[11] S. Schmickl, T. Faseth, and H. Pretl, "An rf-energy harvester and ir-uwb transmitter for ultra-low-power battery-less biosensors," *IEEE Transactions on Circuits and Systems I: Regular Papers*, vol. 67, no. 5, pp. 1459–1468, 2020.

[12] R. Vauche, E. Muhr, N. Tall, A. Haloua, S. Bourdel, J. Gaubert, N. Dehaese, and H. Barthelemy, "Ultra-wideband voltage controlled oscillator with commutable phases for bpsk implementation," in *2015 IEEE 13th International New Circuits and Systems Conference (NEWCAS)*, 2015, pp. 1–4.

[13] F. A. Schoulten, A. A. Mariano, R. Vauche, S. Bourdel, J. Gaubert, N. Dehaese, and H. Barthelemy, "Low power ultra-wide band pulse generator based on a duty-cycled 2-ask emitter," in *2021 19th IEEE International New Circuits and Systems Conference (NEWCAS)*, 2021, pp. 1–4.

[14] M. J. Zhao, B. Li, and Z. H. Wu, "20-pj/pulse 250 mbps low-complexity cmos uwb transmitter for 3–5 ghz applications," *IEEE Microwave and Wireless Components Letters*, vol. 23, no. 3, pp. 158–160, 2013.

[15] J. Ryckaert, G. Van der Plas, V. De Heyn, C. Desset, B. Van Poucke, and J. Craninckx, "A 0.65-to-1.4 nj/burst 3-to-10 ghz uwb all-digital tx in 90 nm cmos for ieee 802.15.4a," *IEEE Journal of Solid-State Circuits*, vol. 42, no. 12, pp. 2860–2869, 2007.

[16] F. C. Commission, *FCC rules and regulations*. Part 15, Jul. 2002.

[17] ETSI, "Etsi en 302 065: Ultra wideband (uwb) technologies for communication purposes," 2010.

[18] IEEE-Std-802.15.4-2020, "Ieee standard for low-rate wireless networks," *IEEE Std 802.15.4-2020 (Revision of IEEE Std 802.15.4-2015)*, pp. 1–800, 2020.

Table IV. Performance Comparison with state-of-the-art works

	JSSC'20 [8]	ITCS'20 [11][&]	JSSC'17 [22]	ISSCC'21 [23]	TMTT'23 [24][*]	This Work[#]
Process (nm)	65	180	28 (FDSOI)	28	28	28 (FDSOI)
Supply Voltage (V)	1.2	1	1	0.9	0.9	1
Core Area (mm^2)	0.22	0.25	0.93	0.154	0.245	-
Modulation Scheme	OOK	TR-IR UWB	2-PPM+BPSK	BPSK	OOK+BPSK	OOK+BPSK
Number of addressed channels (IEEE 802.15.4)	6	5	3	11	12	15
Number of addressed channels (IEEE 802.15.6)	4	5	3	11	8	11
Oscillation Frequency (GHz)	6.5-8	6-8.8	3.5-4.5	3-10	4-9	0.5-13.2
Sidelobes Rejection PSD (dBr)	30	18	20	29	30	21
Amplitude max. (Vpp)	0.46	1	0.9	0.2	0.7	1.1
Leakage Power (μW)	0.38	1.89	174	-	-	14.4
E_{AC} (pJ/pulse)	63	6.2	24	180	140	158
P_C (mW) @PRF=3.9 MHz	0.246	0.026	0.187	0.7	0.546	0.630
P_C (mW) @PRF=15.6 MHz	0.983	0.098	0.268	2.8	2.184	2.478

[&]Double Pulse Transmit-Reference, [*]Carrier input from external signal generator, [#]Simulation Results.

[19] IEEE-Std-802.15.6-2012, "Ieee standard for local and metropolitan area networks - part 15.6: Wireless body area networks," *IEEE Std 802.15.6-2012*, pp. 1–271, 2012.

[20] O. R. Sparrow, R. Vauché, N. Dehaese, S. Bourdel, J. Gaubert, I. B. amor, E. Muhr, P. Losco, and O. Fourquin, "High rate uwb cmos transceiver chipset for wban and biomedical applications," *Analog Integrated Circuits and Signal Processing*, vol. 81, no. 1, pp. 215–227, Oct 2014.

[21] F. A. Schoulten, R. Vauche, S. Bourdel, E. Muhr, J. Gaubert, N. Dehaese, H. Barthelemy, and F. Hameau, "Pulse design method for complexity reduction of ieee ir-uwb pulse synthesizers," in *2020 27th IEEE International Conference on Electronics, Circuits and Systems (ICECS)*, 2020, pp. 1–4.

[22] G. de Streel, F. Stas, T. Gurné, F. Durant, C. Frenkel, A. Cathelin, and D. Bol, "Sleeptalker: A ulv 802.15.4a ir-uwb transmitter soc in 28-nm fdsoi achieving 14 pj/b at 27 mb/s with channel selection based on adaptive fbb and digitally programmable pulse shaping," *IEEE Journal of Solid-State Circuits*, vol. 52, no. 4, pp. 1163–1177, 2017.

[23] E. Allebes, G. Singh, Y. He, E. Tiurin, P. Mateman, M. Ding, J. Dijkhuis, G.-J. v. Schaik, E. Bechthum, J. v. d. Heuvel, M. E. Soussi, A. Breeschoten, H. Korpela, Y.-H. Liu, and C. Bachmann, "21.2 a 3-to-10ghz 180pj/b ieee802.15.4z/4a ir-uwb coherent polar transmitter in 28nm cmos with asynchronous amplitude pulse-shaping and injection-locked phase modulation," in *2021 IEEE International Solid- State Circuits Conference (ISSCC)*, vol. 64, 2021, pp. 304–306.

[24] H. Chen, Z. Chen, R. Ou, R. Chen, Z. Wu, and B. Li, "An ieee 802.15.4z-compliant reconfigurable pulse-shaping uwb digital power amplifier in 28-nm cmos," *IEEE Transactions on Microwave Theory and Techniques*, pp. 1–11, 2023.